FRICTION FACTORS AND INTERNAL FLOW LENGTH SCALES OF GAS-SOLID MAGNETICALLY STABILIZED BEDS IN AXIAL FIELDS
Scaling and applications to bed-to-surface heat transfer

by

Jordan Y. HRISTOV

Original scientific paper
UDC: 536.244:66.086
BIBLID: 0354-9836, *9* (2005), 1, 73-98

Friction factors and internal flow length scales of gas-solid magnetically stabilized beds are discussed. Pressure drop and expansion data of beds stabilized by axial magnetic fields are used. The concept of a variable friction factor of fluid-driven deformable packed bed is discussed. Scaling relationships of the internal flow length scale and the bed overall porosity are developed through three approaches: (1) fluidization approach concerning a length scale proportional to the particle size, (2) packed bed approach based on a hydraulic diameters as a length scale, and (3) porous media approach based on the Forchheimer equation. The main result is that the bed length scale ~ε^n, irrespective of the model used, where n is the exponent of the Richardson-Zaki scaling law. These scaling estimates are used to explain the magnetic field effects on bed-to-surface heat transfer coefficients.

Key words: *fluidization, magnetic field stabilized bed, friction factor, scaling, Richardson-Zaki law, bed-to-surface heat transfer coefficients*

Introduction

The paper discusses gas fluidization of ferromagnetic particles in presence of external magnetic fields. The changes in fluidization behaviour of gas-fluidized coarse particles are attractive for many scientists, since the magnetic field creates new regimes that may be employed in different applications [1, 2].

Friction factors of magnetically stabilized beds in axial field and consequent results concerning heat transfer coefficients to immersed surfaces are at issue. The paper is developed as follows. As a first step friction coefficients (Fanning factors) are determined experimentally. The use of Richardson-Zaki law allows to estimate scaling relations between the friction factor and the bed overall porosity. The second step considers scaling relationship about the bed length scale with respect to the internal fluid flow. Three models are used for that: (1) Pipe analogy of fluidized bed defining the Fanning friction factor, (2) Packed bed model with a hydraulic diameter as a length scale, and (3) Forchheimer equation employing the square root of the Darcy's permeability as a length scale.

The results are used to explain the magnetic field effects on bed-to-surface heat transfer coefficients determined experimentally. Modified Re and Nu numbers are developed based on scaling relationships concerning field effects on bed length scales.

Friction factor concept

The drag force of a fluid exerted on a bed of spherical particles [3, 4]:

$$F = A_c \quad P \tag{1a}$$

can be associated to fluid-solids contact area and the fluid kinetic energy:

$$F \quad fS\frac{\rho U^2}{2} \tag{1b}$$

The factor f is related to the contributions of the pressure distribution over the contact area S and the shear drag caused by velocity gradients. For bed of spheres $S = aV = A_cL$, so:

$$\Delta P \quad faL\frac{\rho U^2}{2} \tag{2a}$$

where

$$a \quad \frac{6}{d_p}(1 \quad \varepsilon) \tag{2b}$$

Hence

$$f_0 \quad \frac{d_p}{L}\frac{1}{1 \quad \varepsilon}\frac{\Delta P}{\frac{\rho U^2}{2}} \quad 6f \tag{2c}$$

The expression (2c) allows to derive two relationships [5]:

$$\Delta P \quad C_D\frac{L}{d_p}\frac{\rho U^2}{2} \tag{3a}$$

and

$$\Delta P \quad \xi\frac{\rho U^2}{2} \tag{3b}$$

The factors C_D and ξ are macroscopic parameters related to the friction factor f_0 as follows:

$$C_D \quad f_0\frac{1}{\Phi(\varepsilon)} \tag{4a}$$

and

$$\xi \quad f_0\frac{d_p}{L}\frac{1}{\Phi(\varepsilon)} \tag{4b}$$

These expressions are classical for the fluidization practice and widely encountered in fixed and fluidized bed studies. In general, fluidized beds exhibit heights depending on superficial fluid velocity and particle orientation. A convenient measure of the total pressure drop, a major characteristic value of a fluidized bed, is the dimensionless friction factor f_0 depending on the particle Reynolds number [3]. Its general form is:

$$f_0 \quad B_0 \quad \frac{B_1}{\mathrm{Re}_\mathrm{p}} \tag{5a}$$

Here B_0 and B_1 are coefficients usually determined experimentally. In case of the Ergun's equation eq. (5a) can be presented as [3]:

$$f_0 \quad 1.75 \quad \frac{150}{\mathrm{Re}^*_\mathrm{p}} \tag{5b}$$

The Reynolds number Re^*_p is typically modified by a term related to the bed porosity. For instance, Wentz and Thodos [3, 4] employed:

$$\mathrm{Re}^*_\mathrm{p} \quad \frac{d_\mathrm{p} G}{\mu(1 \quad \varepsilon)} \tag{6a}$$

where G is the superficial mass velocity of the fluid, while the function $\Phi(\varepsilon)$ is suggested as:

$$\Phi(\varepsilon) \quad \frac{\varepsilon^3}{1 \quad \varepsilon} \tag{6b}$$

Magnetic stabilization – facts related to the friction factor problem

The magnetic field assisted fluidization (MFAF) considers fluidization of magnetic solids controlled by external magnetic fields [1, 2]. The strong interparticle magnetic forces (fig. 1– A) hinder the fluidization and the bed exhibits a "meta" stable state *free of bubbles and mixing motions* with *bed expansion* (fig. 1– B) in small steps. The discussion is focussed on this *meta state* termed "magnetically stabilized bed" (MSB). The external field "induces" (fig. 1– C) particle arrangements along the field lines, thus changing the structure of the porous medium and its hydrodynamic performance (fig. 1– D and E).

Generally, MSB does not operate under compression but it expands due to fluid drag forces [2, 6].The MSB is a packed bed related to problems of porous media with deformable structures. The deformable bed packing alters the porosity function $\Phi(\varepsilon)$ and the total friction drag. Information about the friction factors of MSBs is needed for MFAF engineering design. Such information has not been published yet.

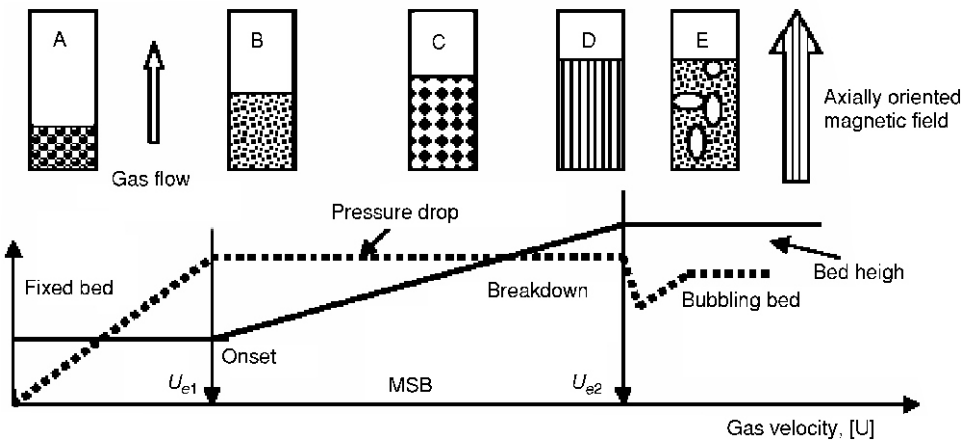

Figure 1. Fluidization in a magnetic field – schematically; case of axial field

Problem formulation

The paper has three goals:

To calculate total friction factors of magnetically stabilized beds created by external magnetic fields with axial orientations (parallel to the fluid flows) and fluidized by air. This implies calculations of the factors C_D and ξ within the velocity range bounded by U_{e1} and U_{e2} (see fig. 1).

To establish scaling functions describing bed length scales evolution during deformation – based on different models of fluid flow through MSB.

To find suitable explanation of the magnetic field effect on bed-to-surface heat transfer coefficients through established *length scale-porosity* relationships.

Experimental and data treatment

Facilities

The experimental unit and materials employed are well described elsewhere [7]. More detailed information is available in [1, 6], but for clarity of explanation a schematic set-up is shown on fig. 2. Iron powder, magnetite and INVAR particles fluidized by air are used. More details are published elsewhere [1, 6].

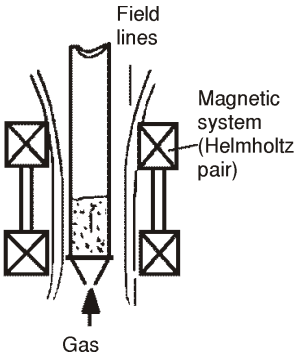

Figure 2. Schematic experimental set-up

Experimental variables and data processing

The experimental data measured are: pressure drop across the bed, bed height, mean particle diameter, gas density (air at ambient conditions). The experimental variables are the superficial gas velocity and the magnetic field intensity. All the data are treated in accordance with eq. (3). The factors C_D and ξ are calculated at each point where MSB exhibits a particular mechanical equilibrium (for detailed comments see [2]).

Development of relationships for the friction factors

Total friction factors – Experimental data

In general, the packed bed friction factor (!!! *The MSB has a fixed bed structure at fixed gas velocity*) depends on the particle Reynolds number, *i. e.* on the superficial fluid velocity. All the results are presented as dimensionless ratios:

$$R_c \quad \frac{C_{\mathrm{i}}}{C_0(\text{at } H \quad 0 \text{ and } U \quad U_{e1})} \tag{7a}$$

and

$$R_\xi \quad \frac{\xi_{\mathrm{i}}}{\xi_0(\text{at } H \quad 0 \text{ and } U \quad U_{e1})} \tag{7b}$$

These dimensionless ratios employ the fact that the friction factors of the initial fixed bed (before the deformation) are easy calculable through the standard relationships (eq. 2c or 5b, for example). The magnetic field does not practically change particle packing in the initial bed [1]. Some examples are illustrated on figs. 3a and 3b, and 4a and 4b where the effects of field intensity, bed height and particle size are demonstrated. The plots indicate three principle characteristics of the total friction factors:

(1) The friction factor ratios decrease 10 times approximately with gas velocity increase.
(2) Initial bed heights have not practically effects on the friction factor evolutions during bed deformation. This independence implies that homogeneous fields create almost similar particle packings within the velocity range of MSB.
(3) The variations of the friction factor ratio are practically independent of the particle size (see fig. 4b). The fact could be attributed to particle arrangements in packed beds (porous media) that are *statistically identical (similar)*. Really the friction factors magnitudes are affected by the particle size (see the caption of fig. 4) but the dimensionless ratio equalizes the differences between them. This can be attributed to the fact that beds in homogeneous axial fields have similar internal structures that are particle size independent.

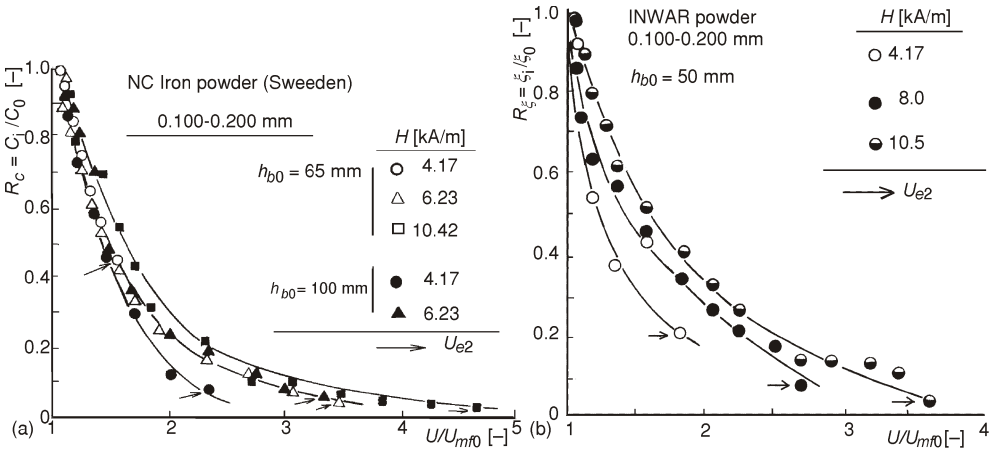

Figure 3. Dimensionless friction factor ratio variations with the dimensionless superficial gas velocity U/U_{mf0} for two high magnetic materijals
(a) Effects of the initial bed height and the field intensity on R_c ratio. Details: C_0 = 465.197 for h_{b0} = 65 mm bed and C_0 = 310.75 for h_{b0} = 100 mm bed; (b) Field intensity effect on R_ξ ratio; ξ_0 = 61683

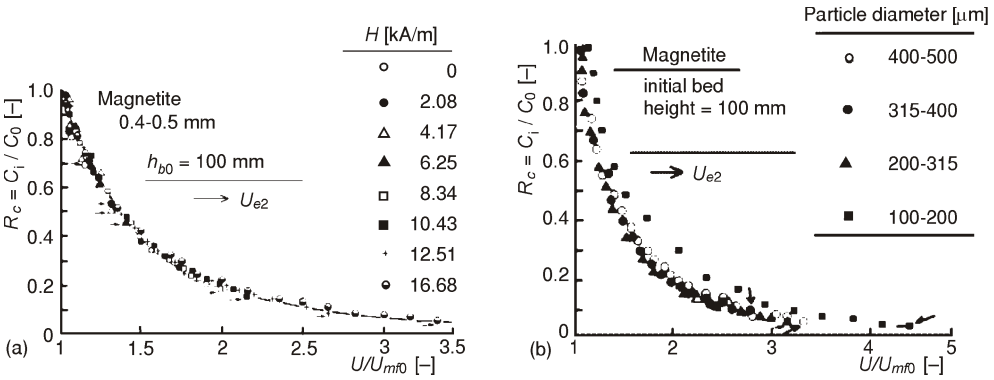

Figure 4. Dimensionless friction factor ratio R_c variations with the dimensionless superficial gas velocity U/U_{mf0}. Magnetite particle beds
(a) Effects of the field intensity. C_0 = 302.32 for h_{b0} = 100 mm bed; (b) Effect of the particle size. Details: C_0 for particle fractions 400-500 μm = 71.39 and for 100-200 μm = 302.32

Fluidization point of view on total friction factors – Data correlations

The friction factor ratio R_c was correlated to the velocity ratio U/U_{mf0} only as:

$$R_c \quad \frac{C_i}{C_0} \quad \Psi \quad \frac{U}{U_{mf0}} \tag{8}$$

- Really, the bed deformation begins at $U = U_{e1}$, so the exact correlation should use the ratio U_{e1} but in axial fields $U_{e1} = U_{mf0}$ [1], so the expression (8) is correct.
- The value U_{mf0} of is easily calculable through numerous relationships available in the literature or could be defined experimentally in absence of a field. Therefore, it can be employed as an *independent velocity scale*.

Two simple forms of eq. (8) are developed:

$$R_c \quad K_L \left(\frac{U}{U_{mf0}} \right)^{M} \quad K_{L0} \tag{9}$$

that is equivalent to the classical relationship (5a), and

$$R_c \quad K_E \exp\left(M_E \left(\frac{U}{U_{mf0}} \right) \right) \quad 1 \qquad K_{E0} \tag{10}$$

Data processing done by *Origin*'s non-linear regression tools yields:

$$R_c \quad 1.13 \left(\frac{U}{U_{mf0}} \right)^{1.879} \qquad 0.041 \tag{11a}$$

and

$$R_c \quad 1.02 \left(\frac{U}{U_{mf0}} \right)^{2.25} \tag{11b}$$

The expressions are based on processing of data obtained with (400-500 μm) magnetite particles arranged as 100 mm deep bed in 65 mm ID glass column. The field intensity was varied within the range (0-16 000 A/m).

Analysis through models

The following analysis considers three standpoints:

Fluidization approach concerning correlations of macroscopic data such as superficial gas velocity, bed height and pressure drop, already used in the previous point and expressed by eqs. (1)-(6).

Packed bed approach employing the bed hydraulic diameter as a length scale.

Porous media standpoint concerning bed permeability through the Forchheimer equation.

Fluidization point of view

The regressions (10) and (11) indicate that we can assume $R_c \sim (U/U_{mf0})^{-2}$ since both exponents are very close to 2. Does the result is surprising? Certainly not, since we

should take into account one special characteristics of bed expansion with stabilized bed mode. As it was illustrated by fig. 1 the pressure drop remains almost constant if the stabilizing field is axially oriented. In fact, the picture in fig. 1 is an idealization, while the real data points oscillate slightly around an average value. This is well known fact and experiential evidences are available elsewhere [1, 7]. If we consider the principles written in eq. (3) and ask a condition of pressure drop independent on the fluid velocity, *i. e.* $P/U = 0$ to be satisfied, the result is:

$$C_D \frac{L}{d_\mathrm{p}} \sim \frac{1}{\frac{\rho U^2}{2}} \quad \text{and} \quad \xi \sim \frac{1}{\frac{\rho U^2}{2}} \tag{12}$$

Therefore, the results seem as predictable ones. Still, there is a question. Both $C_D(L/d_\mathrm{p})$ and ξ are complex characteristics of simultaneously changing bed length and its internal particle re-arrangements. Thus, what happens with the *bed length scale* usually presented by the particle diameter d_p in case of a non-deformable bed? Considering the mass conservation of the solids $L_\mathrm{i}(1-\varepsilon_\mathrm{i}) = L_0(1-\varepsilon_0)$ the ratio R_ξ can be expressed as:

$$R_\xi \quad \frac{\xi_\mathrm{i}}{\xi_0} \quad \frac{C_{D\mathrm{i}} \frac{L_\mathrm{i}}{d_{c\mathrm{i}}}}{C_{D0} \frac{L_0}{d_{c0}}} \quad \frac{C_{D\mathrm{i}}}{C_{D0}} \quad \frac{L_\mathrm{i}}{L_0} \quad \frac{d_{c0}}{d_{c\mathrm{i}}} \quad R_c \quad \frac{1}{1} \quad \frac{\varepsilon_\mathrm{i}}{\varepsilon_0} \quad R_d \tag{13a}$$

where

$$R_d \quad \frac{d_{c0}}{d_{c\mathrm{i}}} \tag{13b}$$

is the *ratio of the internal bed length scales*.

Usually, for a non-deformable bed the internal length scale equals (under a convention) the particle diameter, *i. e.* $d_{c0} = d_\mathrm{p}$.

The expanding bed structure becomes more anisotropic as the fluid-driven deformation develops. The latter implies particle aggregation into strings, extended almost along the field lines and a fluid flowing preferentially through *channels with low hydraulic resistances*. As the fluid velocity approaches the upper limit U_{e2}, the fluid passes primarily through channels thus bypassing the aggregates with porosities almost equal to that of the initial bed – ε_0. This fact indicates that the internal bed length scale varies as the fluid flow increases.

Length scale evolution-particle diameter related scale

The following analysis employs some assumptions that have to clarify the explanation. First, let us assume the porosity function $\Phi(\varepsilon)_\mathrm{i} = 1 - \varepsilon_\mathrm{i}$ as in eq. (2). Second, we can use the recently proved scaling of the MSB expansion by the Richardson-Zaki power

laws $U/U_t \sim \varepsilon^n$ [8] (see also [1, 2]). Third, both the particle terminal velocity U_t and the minimum fluidization velocity in absence of a field U_{mf0} *are field independent values.* As a result, we can combine the scaling estimation (12) with the Richardson-Zaki law [8] and (13a) can be re-written as:

$$R_\xi \quad R_c \quad \frac{d_\mathrm{p}}{d_{ci}} \quad \frac{1 \quad \varepsilon_0}{1 \quad \varepsilon_\mathrm{i}} \sim \frac{1}{\left(\dfrac{U}{U_{mf0}}\right)^2} \sim \frac{1}{\varepsilon_\mathrm{i}^{2n}} \tag{14a}$$

where

$$R_c \quad \frac{f_0 \Phi(\varepsilon)_\mathrm{i}}{f_0 \Phi(\varepsilon)_0} \quad R_{f0} \frac{\Phi(\varepsilon)_\mathrm{i}}{\Phi(\varepsilon)_0}$$

$$\frac{d_\mathrm{p}}{d_{ci}} \underbrace{\frac{L_0}{L_\mathrm{i}} \frac{1 \quad \varepsilon_0}{1 \quad \varepsilon_\mathrm{i}}}_{1} \frac{\Phi(\varepsilon)_\mathrm{i}}{\Phi(\varepsilon)_0} \quad \frac{d_\mathrm{p}}{d_{ci}} \quad \frac{1 \quad \varepsilon_0}{1 \quad \varepsilon_\mathrm{i}}^2 \quad \frac{\varepsilon_\mathrm{i}}{\varepsilon_0}^3 \tag{14b}$$

so we have:

$$R_\xi \quad \frac{d_\mathrm{p}}{d_{ci}}^2 \quad \frac{1 \quad \varepsilon_0}{1 \quad \varepsilon_\mathrm{i}}^3 \quad \frac{\varepsilon_\mathrm{i}}{\varepsilon_0}^3 \sim \frac{1}{\varepsilon_i^{2n}} \quad \frac{d_\mathrm{p}}{d_{ci}}^2 \sim \frac{1}{\varepsilon_i^{2n}} \frac{1 \quad \varepsilon_\mathrm{i}}{1 \quad \varepsilon_0}^3 \quad \frac{\varepsilon_0}{\varepsilon_\mathrm{i}}^3 \tag{15}$$

The porosity ε_0 is within the range $0.39 < \varepsilon_0 < 0.5$ while ε_i varies with the interval $0.5 < \varepsilon_0 < 0.7$. Hence, looking at the order of magnitudes in eq. (15) we can decide that order of magnitudes $\mathrm{O}(1-\varepsilon) = \mathrm{O}(\varepsilon)$ are within the interval of variations. Thus, we can approximate the second term as $(1-\varepsilon)_\mathrm{i}/(1-\varepsilon)_0 \quad \varepsilon_\mathrm{i}/\varepsilon_0 \quad 1$, so the result from eq. (15) is:

$$\frac{d_\mathrm{p}}{d_{ci}} \sim \frac{1}{\varepsilon_\mathrm{i}^n} \tag{16}$$

The data of Rosensweig [9] and Foscolo *et al.* [10] indicate that $n \quad 3$, while the recent results of Hristov [1, 2] indicate that:

$$n = n_0 - p(H/Ms) \tag{17}$$

The second term of eq. (17) represents the field effect on the Richardson-Zaki exponent through the dimensionless field intensity (*H/Ms*). For iron, magnetite and nickel the ratio (*H/Ms*) varies from 10^{-2} up to10^{-1}. In case of artificial magnetite (ammonia catalyst "H. Topsoe" KM-1) the coefficients of eq. (17) are $n_0 \quad 2.84$ and $p = 0.313$ respectively [2]. Therefore, the scaling law derived from eqs. (16) and (17) is:

$$d_{ci} \sim d_\mathrm{p} \varepsilon_\mathrm{i}^{n_0 \quad p(H/Ms)} \tag{18}$$

Packed bed approach

Logically, we can expect that the expanding bed volume is a result of increased distances between the particles. In magnetically stabilized bed two interrelated phenomena occur:

The particles are packed in aggregates with porosity close (or almost equal) to that of the initial packed bed.

The channels between the aggregates become longer as the deformation occurs. This implies increasing channel lengths and wetted surfaces due to fluid drag forces.

Common approach for fluid flow through packed bed is to use eq. (3a) with the bed *hydraulic diameter as a length scale* [11, 12]:

$$D_H \quad 4\frac{\text{wetted volume}}{\text{wetted surface}} \quad 4\frac{V}{S} \tag{19a}$$

where for bed of isotropic packing [12] it is:

$$D_{H0} \quad \frac{4}{6}d_{\mathrm{p}}\frac{\varepsilon_0}{1 \quad \varepsilon_0} \tag{19b}$$

With reference to the result presented by the scaling estimate (13a and b, 14a) we have:

$$R_\xi \quad \frac{C_{D\mathrm{i}}}{C_{D0}}\frac{L_{\mathrm{i}}}{L_0}\frac{D_{H0}}{D_{H\mathrm{i}}} \sim \frac{1}{\varepsilon^{2n}} \tag{20a}$$

where

$$\frac{D_{H0}}{D_{H\mathrm{i}}} \quad \frac{V_0}{V_{\mathrm{i}}}\frac{S_{\mathrm{i}}}{S_0} \quad \frac{A_c\varepsilon_0 L_0}{A_c\varepsilon_{\mathrm{i}}L_{\mathrm{i}}}\frac{\Pi_{\mathrm{i}}L_{\mathrm{i}}}{\Pi_0 L_0} \quad \frac{\varepsilon_0}{\varepsilon_{\mathrm{i}}} \quad \frac{\Pi_{\mathrm{i}}}{\Pi_0} \tag{20b}$$

with wetted perimeters Π_0 and Π_{i} respectively. Expression (20a) becomes:

$$R_\xi \quad \frac{C_{D\mathrm{i}}}{C_{D0}}\frac{L_i}{L_0} \quad \frac{\varepsilon_0}{\varepsilon_i} \quad \frac{\Pi_{\mathrm{i}}}{\Pi_0} \quad \sim\frac{1}{\varepsilon^{2n}} \tag{21}$$

Assuming a bed consisting of N_i straight channels of diameter $C_{n\mathrm{i}}$ and length L_{i} and that $\varepsilon_{\mathrm{i}} = \varepsilon_0$(aggregates) + $\Delta\varepsilon_{\mathrm{i}}$(channels), eq. (21) can be expressed as:

$$\frac{C_{D\mathrm{i}}}{C_{D0}} \quad \frac{2\pi C_{n\mathrm{i}}N_{\mathrm{i}}}{2\pi C_{n0}N_0} \sim\frac{1}{\varepsilon^{2n}} \qquad \frac{C_{D\mathrm{i}}}{C_{D0}} \quad \frac{N_{\mathrm{i}}}{N_0} \quad \frac{C_{n\mathrm{i}}}{C_{n0}} \sim\frac{1}{\varepsilon^{2n}} \tag{22}$$

Here $C_{n\mathrm{i}}$ and C_{n0} denote the channels diameters in the deformed and initial packed bed respectively.

Two situations can be suggested: (1) The *number of the channels remain unchanged* ($N_i = N_0$) and the fluid drag forces change *only their diameters and lengths*; (2) The number of the channels varies ($N_i \quad N_0$) with the bed deformations.

According to the first hypothesis the channel diameter and following eq. (22), it is possible to scale (with a mean value of $n \quad 3$):

$$\frac{C_{Di}}{C_{D0}} \quad \frac{C_{ni}}{C_{n0}} \sim \frac{1}{\varepsilon^{2n}} \tag{23}$$

The problem that arises is about the ratio (C_{Di}/C_{D0}). The scaling estimates (12a and b) include a fixed value of the bed length scale d_p and a macroscopically measured bed depth L_i that permits to calculate the values of C_{Di}. Thus, replacing d_p by D_H in eq. (3a) we receive a second variable that does not allow to calculate directly C_{Di}. Equation (22b) teaches that:

$$D_{Hi} \sim D_{H0}\,\varepsilon_i \tag{24}$$

where D_{H0} can be calculated from eq. (19b).

Hence, the result from eq. (22) is:

$$\frac{C_{Di}}{C_{D0}} \sim \frac{1}{\varepsilon^{2n}} \tag{25}$$

that confirms the general scaling estimates (11) and (12). Therefore, the ratio of the channel diameters is about unity (C_{ni}/C_{n0}) ~ 1. Thus, the suggestion $N_i = N_0$ leads to a result indicating that the fluid drag only extends the channels but does not affect their diameters (this also implies increasing wetted surfaces of the channels).

The second hypothesis ($N_i \quad N_0$) leads to:

$$\frac{N_i}{N_0} \quad \frac{C_{ni}}{C_{n0}} \sim 1 \quad \frac{S_i}{S_0} \sim \frac{\varepsilon_i}{\varepsilon_0} \tag{26}$$

i. e. the wetted surface of the bed increases with the increase of the porosity. This result is physically more general and includes also the case when (C_{ni}/C_{n0}) ~ 1.

Brief comments on the results from fluidization and packed bed approaches

Both examples employing the so-called tube (pipe) analogy to calculate bed friction factors provide similar results. In fact, these models operate with effective parameters well describing (approximating) experimental data. The two results, eq. (18) and (24), indicate that when the porosity approaches unity ($\varepsilon \quad 1$) the internal bed length

scales become d_{ci} d_p and D_{Hi} $D_H = D$ respectively. The former results strictly indicate that the particle diameter is a length scale in dilute systems with porosity close to unity. As the porosity decreases the size of cavities and the throats of the channels between particles become more important for the fluid flow than the particle diameter. Actually, the real length scale is – see eqs. (4a) and (6b), $d^* = d_p/\Phi(\varepsilon)$. Thus, the real definition of (see eq. (13b) is:

$$R_d \quad \frac{d_p}{d_{ci}} \frac{1 \quad \varepsilon_i}{1 \quad \varepsilon_0} \tag{27}$$

On the other hand, the general model employing hydraulic diameters gives $R_d = D_{H0}/D_{Hi}$.

Taking into account that for non-deformed bed (the initial bed packing) the hydraulic diameter is [11, 12] given by eq. (19b) the hydraulic diameter of a deformable bed in accordance with eq. (24) can be expressed as:

$$D_{Hi} \sim D_{H\,0} \quad \frac{\varepsilon}{\varepsilon_0} \qquad D_{Hi} \quad \frac{\varepsilon_i}{6(1 \quad \varepsilon_0)} d_p \tag{28a}$$

Introducing the field effect on the Richardson-Zaki exponent n – see eq. (17), we have:

$$D_{Hi} \quad \frac{d_p}{6(1 \quad \varepsilon_0)} \quad \frac{U}{U_t} \quad ^{\frac{1}{n_0 \quad p(H/Ms)}} \tag{28b}$$

Porous media approach

The well known one-dimensional Forchheimer equation of a fluid flow through a saturated porous medium [13-17] is:

$$\frac{\Delta P}{L} \quad \frac{\mu}{K} U \quad \frac{F \rho_g}{\sqrt{K}} U^2 \tag{29a}$$

where K is the porous media permeability.

Rearranging eq. (29a) as:

$$\frac{\Delta P}{L} \frac{1}{\rho_g U^2} \frac{\sqrt{K}}{F} \quad f \quad \frac{1}{\mathrm{Re}} \quad 1 \tag{29b}$$

we obtain *friction factor – Reynolds number* type of correlation which is "presumably" universal – and resembles eq. (5b) – with $\mathrm{Re} \quad F(\rho_g K^{1/2} \big/ \mu) U$.

Algebraic solution 28

Equation (29a) with $1/K^{1/2}$ Z can be expressed as:

$$-\Delta P = L(\mu U Z^2 + F\rho_g U^2 Z) \tag{29c}$$

The general condition that can be imposed on eq. (29), in case of expanding magnetizable bed, is a *constant pressure drop*. This implies that the derivative of the right-hand side with respect to the velocity U has to equal to zero.

The condition $\partial(\Delta P)/\partial U$ 0 provides $Z_1 = 0$ and a non-trivial solution Z_2 as:

$$Z_2 \quad Z \qquad \frac{F\rho_{\mathrm{f}}}{\mu_{\mathrm{f}}} U \; 1 \; \frac{L_{\mathrm{i}}}{\dfrac{\partial L_{\mathrm{i}}}{\partial U} U \quad L_{\mathrm{i}}} \qquad \frac{F\rho_{\mathrm{f}}}{\mu_{\mathrm{f}}} U(1 \quad \beta) \tag{30}$$

In other words, the first term of eq. (30) gives that $(1/Z)^2 = K$ $1/U^2$. Taking into account the mass conservation of the solid phase $L_{\mathrm{i}}(1 - \varepsilon_{\mathrm{i}}) = L_0(1 - \varepsilon_0)$ the derivative $\partial L_i / \partial U$ can be expressed as:

$$\frac{\partial L_{\mathrm{i}}}{\partial U} \quad \frac{\partial L_{\mathrm{i}}}{\partial \varepsilon}\frac{\partial \varepsilon}{\partial U} \qquad L_0 \frac{1 \quad \varepsilon_0}{(1 \quad \varepsilon_{\mathrm{i}})^2}\frac{\partial \varepsilon}{\partial U} \tag{31}$$

The substitution of $\partial L_{\mathrm{i}}/\partial\varepsilon$ and $L_{\mathrm{i}}/\partial U$ from eq. (31) and $\partial\varepsilon/\partial U$ through $U/U_t = \varepsilon^n$ [8, 18] in eq. (30) yields $\beta = L_{\mathrm{i}}/[L_{\mathrm{i}} + U(\partial L/\partial U)] = n(1 - \varepsilon)/\varepsilon$. Therefore, the solution is:

$$Z \qquad \frac{F\rho_{\mathrm{f}}}{\mu_{\mathrm{f}}} U \; 1 \; \frac{n(1 \quad \varepsilon}{\varepsilon} \qquad |Z| \quad F\frac{\rho_{\mathrm{f}}}{\mu_{\mathrm{f}}} U_t \varepsilon^n \; 1 \quad \frac{n(1 \quad \varepsilon)}{\varepsilon} \tag{32}$$

Since $K = (1/Z)^2$ the negative sign of Z in eq. (32) is not a confusing result (see subsubsection Comments on the negative sign of Z) and we have a positive permeability that is physically correct:

$$K \quad \frac{1}{Z}^2 \qquad \frac{1}{F}\frac{\mu}{\rho}\frac{1}{U}^2 \qquad \frac{\varepsilon}{n(1 \quad \varepsilon) \quad \varepsilon}^2 \tag{33a}$$

Equation (33a) allows to express the porous bed length scale as:

$$\sqrt{K} \quad \left|\frac{1}{Z}\right| \quad \frac{\mu_{\mathrm{f}}}{F\rho_{\mathrm{f}}}\frac{1}{U_t}\frac{1}{\varepsilon^n} \quad \frac{\varepsilon}{n(1 \quad \varepsilon) \quad \varepsilon} \tag{33b}$$

Similar result:

$$K \quad \frac{1}{Z}^2 \qquad \frac{1}{F}\frac{\mu}{\rho}\frac{1}{U}^2 \tag{33c}$$

can be developed faster if a derivative $\partial P/\partial U = 0$ from the left-hand side of eq. (29a) is taken. In this case the variations of the bed height with the velocity $\partial L/\partial \varepsilon$ are not considered.

Comments on the negative sign of Z in eq. (32)

The negative sign of the root Z derived in eqs. (31) and (32) needs special comments. The fluid-driven expansion of MSB and the non-magnetic A powders (according to Geldart [18]) are typical examples of deformable porous media *obeying conditions of constant (velocity independent) pressure drops.* Obviously the result of eq. (32) is $K = (1/Z)^2$, so the permeability is positive and no contradiction with the classic porous media results exists. Let us explain why the sign of Z is negative and that the positive permeability is not a result of mathematical manipulations. Figure 5 illustrates typical *pressure drop- fluid velocity* curves in two versions. The version A demonstrates the total pressure

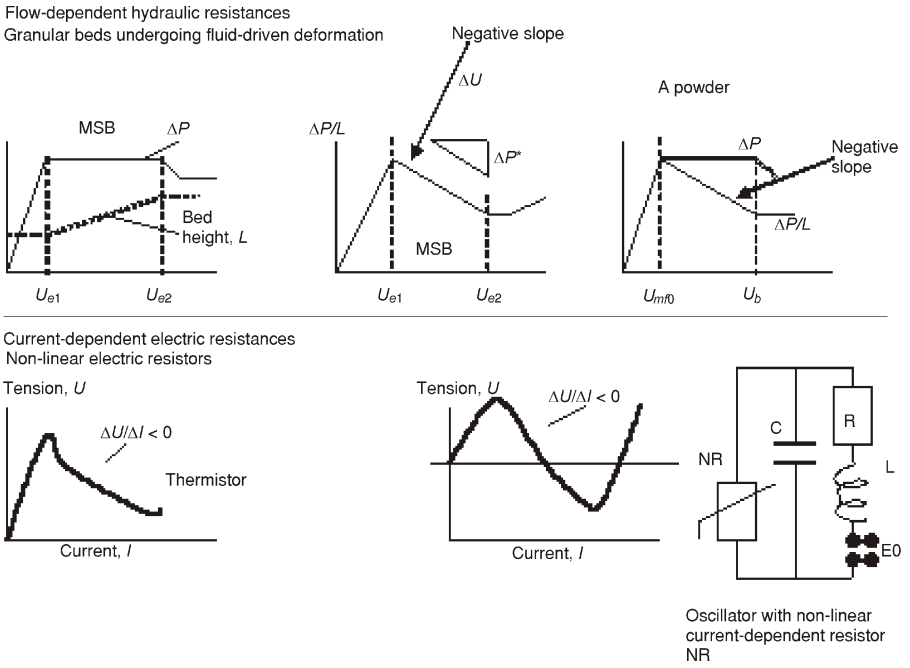

Figure 5. Negative differential resistances demonstrated by homogeneously expanding fluidized beds with strong interparticle forces and non-linear electric resistances. Shematic presentations and analogies
Upper half: Flow dependent hydraulic resistances – Version A – MSB (left) and A powders (right) with positive static resistances. Version B (center) – Negative differential resistance of deforming bed. Present author interpretation
Bottom half: Examples of negative differential resistances exhibited by current-dependent non-linear resistors. According to Philippow [20]

drop evolution with the increasing fluid velocity. Version B presents the pressure drop gradient $P^* = \Delta P/L$ as in the case of the Forchheimer equation. Hence, if ΔP remains practically unchanged while L increases the function $P^* = \phi(U)$ will exhibit a negative slope $\partial P^*/\partial U$. A system exhibiting such negative slope has a *negative differential resistance*. At a fixed point of the descending curve the ratio P^*/U define a *positive static bed resistance* that is proportional to $1/K$, while the *differential resistance* $\partial P^*/\partial U$ is negative. This fact is well-known from the non-linear electrical circuits [19] and especially from those describing thermistors (see fig.5) as current-dependent resistors and electrical oscillators with non-linear resistors. Negative differential resistance is a strong indicator that the system is at a transition regime and tends to a point where it may "jump" into a new stable state. Therefore, the differential resistance $\partial P^*/\partial U$ 0 characterizes the transition regime between the naturally stable initial fixed bed (with $\partial P^*/\partial U$ 0) and the fluidized state. The expanding particle bed, irrespective of the type of the stabilizing forces (native cohesion or induced magnetic forces), is a system approaching its instability point at $U = U_{mf}$ (with bubbling) as the fluid velocity increases. It is well known that magnetically controlled beds in axial fields [1] do not change their heights after the fluidization onsets as the fluid velocity is increased. From the standpoint of the present analysis at U U_{mf} the gradient $P^* = \Delta P/L$ is practically constant (or slightly positive) that results in $\partial P^*/\partial U$ 0 or $\partial P^*/\partial U$ 0. The latter means that the bed dynamic resistance becomes almost positive beyond $U = U_{mf}$.

Both the fixed and the fluidized bed can be considered as two stable regimes either from thermodynamic or mechanical point of view. The interparticle forces can alter the transition between them and the "life" (the velocity range where it exists) of this "shift" depends on their strengths. Therefore, *low bed cohesion – fast transition* into a fluidized bed and *vice versa*. The magnetic stabilization is just an artificially created "long" transition from fixed into fluidized bed. In the case of A powders the native cohesion plays the same role. The *negative differential resistance* of particle beds undergoing fluidization is a problem attractive for investigation and research studies, except the present comments, are not published yet.

The negative sign of Z has more simple but formalistic explanation. The negative differential resistance is equivalent to the first derivative of the friction factor with respect to the velocity. The general definition of the Fanning friction factor (see eqs. 2c, 5a, 5b, and 29b) defines it as a *flow-dependent hydraulic resistance* or more exactly as a *positive static* (specific) hydraulic resistance (per unit bed length). Thus, for rigid porous media the differential resistance is $\partial f/\partial U$ Re $\sim -1/U^2$ while for deformable porous structures $f/u \sim -1/U^m$ but the exponent m should depend on the fluid flow-bed deformation mechanism. In case of MSBs in axial fields $f/\partial u \sim -1/U^3$ – see eq. (12).

Simplification of the porosity function 28

The applications of the porosity function directly in Re and Nu numbers result in "clumsy" formulae. An attempt to simply $\Phi(\varepsilon)$, for engineering use through expansion as a power series (function ***series*** of Maple 7 – symbolic mathematics) yields:

$$\Phi(\varepsilon) \quad \frac{1}{\varepsilon^n} \quad \frac{\varepsilon}{n(1 \quad \varepsilon) \quad \varepsilon} \quad \frac{1}{n}\varepsilon^{(n \ 1)} \quad \frac{2}{n^2}\varepsilon^{(n \ 2)} \ldots \quad O(\varepsilon^6) \tag{34a}$$

and especially for $n = 3$:

$$\Phi(\varepsilon) \quad \frac{1}{3}\varepsilon^{2} \quad \frac{2}{9}\varepsilon^{1} \quad \frac{4}{27} \quad \frac{8}{81}\varepsilon \quad \ldots \tag{34b}$$

Taking into account that $0.4 \quad \varepsilon \quad 0.8$ and the order of magnitudes (O) of the terms of the series we can use the first terms only:

$$\Phi(\varepsilon) \quad \frac{1}{n}\varepsilon^{(n \ 1)} \tag{34c}$$

This approximation is that is close to $\Phi(\varepsilon) \quad 1/\varepsilon^n$ coming from eq. (33c).

Comments on the friction factor evolution with the porosity increase

According to eq. (12) and the comments in subsubsection Comments on the negative sign of Z, the friction factors of MSB decrease faster with the fluid velocity unlike in cases of rigid beds, *i. e.* the derivative $\partial f/\partial U \quad 1/U^3$ for expanding bed while for a rigid bed it is $\partial f/\partial U \quad 1/U^2$. The bed friction factor of the Forchheimer equation (29b) through the results in eqs. (33) taking into account that $U_t/U = 1/\varepsilon^n$ is:

$$\mathrm{Re} \quad \frac{1}{n}\varepsilon \quad \frac{2}{n^2}\varepsilon^2 \quad \ldots \quad O(\varepsilon^{6 \ n}) \tag{35a}$$

$$f \quad \frac{1}{\mathrm{Re}} \quad 1 \quad 1 \quad \frac{U_t}{U}\Phi(\varepsilon)^{1} \quad 1 \quad \frac{1}{\frac{1}{n}\varepsilon \quad \frac{2}{n^2}\varepsilon^2} \tag{35b}$$

Both the approximation (34c) and the field effect on through eq. (17) provide a more simple expression:

$$f \quad 1 \quad \frac{n}{\varepsilon} \quad 1 \quad \frac{n_0 \quad p\,\frac{H}{Ms}}{\varepsilon} \tag{35c}$$

Therefore, the friction factor decreases as the porosity increases that is a physically correct result. In the same time at fixed values of ε an increase of field intensity leads to reduced friction factors. The latter is consistent with the fact of preferential flow through axially oriented channels. The use of oversimplified function $\phi(\varepsilon) \quad 1/\varepsilon^n$ yields unrealistic result $f \quad 2$.

Case of independent coefficients of Darcy-Forchheimer equation

We now turn to the Darcy-Forchheimer equation in its general form:

$$\frac{\Delta P}{L} \quad aU \quad bU^2 \tag{36}$$

where the coefficients a and b are experimentally defined values. Generally, we may suggest that the coefficients a and b in eq. (36) are independent unlike the specific case expressed by eq. (29a) where both of them are expressed through the permeability K.

The general question is: If the pressure drop, especially the derivative $\partial(\Delta P)/\partial U$, is preliminary defined by experimental results, what functional relationship should satisfy the coefficients a and b if the bed expands (fluid-driven expansion) and the Richardson-Zaki Law is valid.

Let differentiate both sides of eq. (29a) with respect to the velocity U:

$$\frac{\partial \Delta P}{\partial U} \quad a \quad L_{\mathrm{i}} \quad U\frac{\partial L_{\mathrm{i}}}{\partial U} \quad b \quad 2L_{\mathrm{i}}U \quad U^2\frac{\partial L_{\mathrm{i}}}{\partial U} \tag{37}$$

Generally the slope $\Delta P/\Delta U$ is negative (see fig. 5) so we have $\Delta P/\Delta U = m \quad 0$ and the results is

$$m \quad \frac{a}{bU} \quad 1 \quad (bU) \quad L_{\mathrm{i}} \quad U\frac{\partial L_{\mathrm{i}}}{\partial U} \quad bUL_{\mathrm{i}} \tag{38}$$

We have options to vary the conditions affecting the terms of eq. (38) and consequently the functional relationship that should be satisfied by the coefficients a and b. The main options are: (1) to vary the value of m; (2) to control the last term of eq. (38b) representing the bed rheology. The further analysis considers the term $L_{\mathrm{i}} \quad U(\partial L_{\mathrm{i}}/\partial U$ in eq. (38) representing bed rheology during deformation. Taking into the results (31) and (32) and introducing the variable β we can read eq. (38) as:

$$m \quad \frac{a}{\beta} \quad (bU) \quad \frac{1}{\beta} \quad 1 \quad L_{\mathrm{i}} \tag{39}$$

The solution of eq. (39) with respect the coefficient b is:

$$b \quad \frac{1}{U} \quad \frac{m}{L_{\mathrm{i}}} \quad \frac{a}{\beta} \quad \frac{\beta}{1 \quad \beta} \tag{40}$$

This is the condition that should be satisfied by the coefficients a and b if $\partial(\ P)/\partial U$ is preliminarily defined. This general result will be discussed below in two specific cases.

Case 1. Fluid velocity independent pressure drop $m = 0$ (axial fields)

This is the dominating practical case and the condition $m = 0$ leads to:

$$b \quad \frac{1}{U} \quad \frac{a}{1 \quad \beta} \tag{41}$$

However the Darcy term defines the coefficient a as a = μ/K so from eqs. (41) and (36) we have:

$$\frac{\Delta P}{L} \quad aU \quad \frac{a}{1 \quad \beta}U \quad \frac{\Delta P}{L} \quad aU \quad 1 \quad \frac{1}{1 \quad \beta} \quad \frac{\mu}{K}U \quad 1 \quad \frac{1}{1 \quad \beta} \tag{42}$$

A substitution of $\beta = n(1 - \varepsilon)/\varepsilon$ and the Richardson-Zaki law into eq. (41) yields the coefficient b:

$$b \quad \frac{\mu}{K}\frac{1}{U_t \varepsilon^n}\frac{1}{1 \quad \frac{n(1 \quad \varepsilon)}{\varepsilon}} \tag{43}$$

The last arrangement of eq. (42) allows obtaining the friction factor as follows:

$$\frac{\Delta P}{\rho U^2}\frac{1}{L}\sqrt{K} \quad \frac{\mu}{K}\sqrt{K}\frac{1}{\rho U} \quad 1 \quad \frac{1}{1 \quad \beta} \tag{44a}$$

and

$$f \quad \frac{1}{\mathrm{Re}} \quad \frac{\beta}{1 \quad \beta} \tag{44b}$$

where $f = (\Delta P / \rho U^2)(1/L)K^{1/2}$ and $\mathrm{Re} \quad UK^{1/2}/\nu$ are the friction factor and Reynolds number defined in a classical manner in accordance with the Darcy-Forchheimer equation in a form presented by eq. (29a). Equation (44a) allows reading the permeability K as :

$$K \quad \frac{L}{\Delta P}\mu U \quad \frac{\beta}{1 \quad \beta} \qquad K \quad \frac{L}{\Delta P}\mu U_t \varepsilon^n \quad \frac{n(1 \quad \varepsilon)}{\varepsilon \quad n(1 \quad \varepsilon)} \tag{45}$$

as ε 1 (empty tube) the permeability approaches the Darcy definition $K \quad \mu U \quad P/L$)

Case 2. General case with $m \quad 0$

The solution of eq. (39) with $m \quad 0$ yields :

$$b \quad \frac{1}{U} \quad \frac{m}{L_i} \quad \frac{a}{\beta} \quad \frac{\beta}{1 \quad \beta} \tag{46}$$

This allow to present the pressure drop $\Delta P/L_i$ as :

$$\frac{\Delta P}{L_i} \quad a \quad \frac{\beta}{1 \quad \beta} \quad U \qquad \frac{\beta}{1 \quad \beta} \quad mU \tag{47}$$

at $m = 0$, the results is eq. (42).

The solution of eq. (47) with respect to the coefficient $a = \mu/K$ is:

$$a \qquad \frac{\Delta P}{L_i}\frac{1}{U}\frac{1 \quad \beta}{\beta} \qquad K\frac{\mu}{\dfrac{\varepsilon \quad n(1 \quad \varepsilon)}{n(1 \quad \varepsilon)}\dfrac{\Delta P}{L_i}\dfrac{1}{U} \quad m} \tag{48}$$

as $\varepsilon \quad 1$ and $m \quad 0$ (empty tube) and the permeability approaches the Darcy definition $K \quad \mu U/(\Delta P/L)$.

Heat transfer applications of the results

Bed-to-surface heat transfer coefficients h_w in magnetically stabilized beds have been determined experimentally with probes of three uncomplicated geometries – plates, cylinders, and spheres. The experimental data were re-examined in [20, 21]. The reconstruction of the experiments [20, 21] provides an important fact irrespective of the field line orientation and the probe configuration: during bed deformation the value of h_w *increases monotonously* and reaches its maximum in the marginal zone of transition from stabilized into fluidized bed. Two examples are shown on figs. 6 and 7. The value of max h_w depends on the field intensity. The following relationship was developed [20, 21] on the basis of experimental data published in literature:

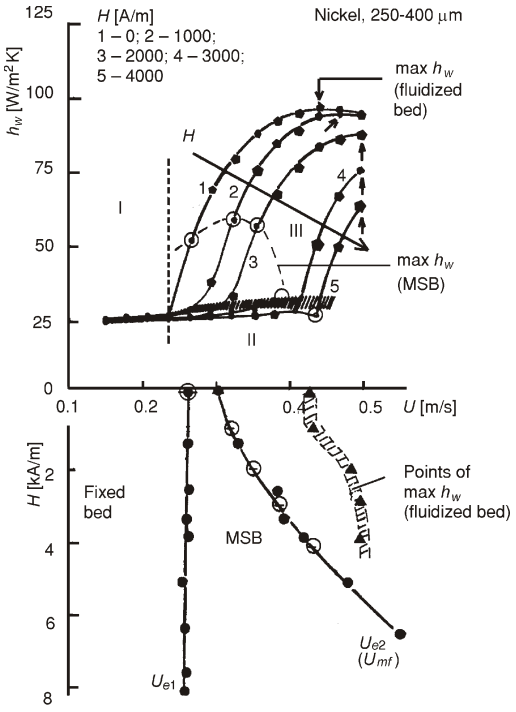

Figure 6. Field effect on bed-to-surface heat transfer coefficient with a reconstructed phase diagram. Adapted from [23] and developed here. Original data of Amaldos [26]
Upper half – $h_w = f(U)$ at fixed field intensity – Magnetization first mode (see definition in [1, 22, 23]);
Bottom half – Reconstructed phase diagram

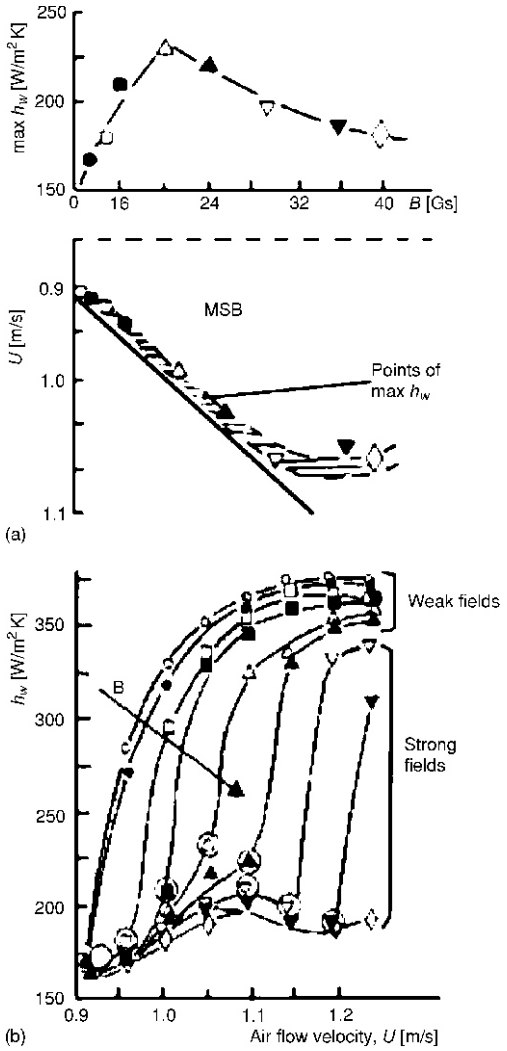

Figure 7. Field effect on bed-to-surface heat transfer coefficients. Data based on the measurements of Neff and Rubinsku [27]
(a) Variations with the fluid velocity in MSB regime. Data extracted and treated in [21]; (b) Original data of Neff and Rubinsky: Labels (B, gauss): ○ – 0; ● – 6.20; □ – 12.28; ■ – 15.25; △ – 21.40; **▲** *– 24.44;* **▽** *– 30.52; ▼ – 36.59; ◇ – 39.63*

$$\mathrm{Nu_p} \quad \frac{h_w d_\mathrm{p}}{k_g} \quad A_0 \,\mathrm{Re_p^{\,m}}\,\mathrm{Pr}^{0.8}\sqrt{\mathrm{Ar}}\;\frac{k_g}{k_\mathrm{p}} \quad 1 \quad \frac{H}{Ms} \tag{49}$$

The last term represents the effects of field intensity and magnetic properties of solids through the dimensionless intensity *H/Ms* (introduced in [23]; see also [2]). Equation (49) was derived as settlement of compromise [20, 21] due to absence of reliable data concerning bed porosity published in the literature.

The geometry of the immersed surface (probe) does not affect significantly the overall heat transfer coefficients [20, 21]. The following analysis attends to correlations between heat transfer coefficients to plate-type probes and deformation characteristics of MSB. Let us consider an immersed probe (plate) oriented vertically along both the field lines and gas flow. Beckerman and Viskanta [24] described by the Forchheimer equation a momentum boundary layer (of thickness δ) along the impermeable surface (probe or column wall).The single parameter characterizing the flow is a modified Reynolds number Re $(U_c K^{1/2}/\nu)F$, where U_c [$(\mathrm{d}P/\mathrm{d}x)K]/\mu_f$ – is a characteristic Darcian velocity. The thermal boundary layer of thickness δ_T is governed by a modified Prandtl number $\mathrm{Pr} = \nu/\alpha_{\mathrm{eff}}F$. The heat transfer rate at the impermeable wall (of the probe) are represented as Nusselt number [24]:

$$\mathrm{Nu} \quad \frac{h_w\sqrt{K}}{k_{\mathrm{eff}}} \tag{50}$$

If the result (32) and the approximations (34c) are applied the corresponding Reynolds and Nuselt numbers are:

$$\mathrm{Re} \quad \frac{U_c\sqrt{K}}{\nu}F \quad \frac{U_c}{U_t} \quad \frac{1}{n}\frac{1}{\varepsilon^{n\ 1}} \quad \frac{U_c}{U} \quad \frac{1}{n}\varepsilon \tag{51}$$

and

$$\mathrm{Nu} \quad \frac{h_w\sqrt{K}}{k_{\mathrm{eff}}} \quad \frac{h_w}{k_{\mathrm{eff}}}\frac{1}{F}\frac{\nu}{U_t} \quad \frac{1}{n}\frac{1}{\varepsilon^{n\ 1}} \tag{52}$$

For an undeveloped thermal boundary layer at very small Pr numbers (the case of MSB is the same, *i. e.* $\delta_T \gg \delta$. The latter is equivalent to 0 Pr 1 (for values $0.5 < \mathrm{Pr} < 1$ of in MSB, see [22]). In this case the thermal boundary layer is $\delta_T \quad 6.0(x/\mathrm{Re}\,\mathrm{Pr}\,u_\infty)^{1/2}$, that yields:

$$\mathrm{Nu} \quad \frac{1}{\pi x}\sqrt{\mathrm{Re}\,\mathrm{Pr}\,u_\infty} \tag{53}$$

Taking into account the expressions (52) and neglecting all parameters being constants we read:

$$\mathrm{Nu} \quad \frac{1}{\pi x}\sqrt{\mathrm{Re}\,\mathrm{Pr}\,u_\infty} \quad \frac{h_w}{k_{\mathrm{eff}}}\frac{1}{F}\frac{\nu}{U_t} \quad \frac{1}{n}\frac{1}{\varepsilon^{n\ 1}} \quad \sqrt{\frac{U_c}{U}\ \frac{1}{n}\varepsilon} \tag{54a}$$

and

$$h_w \quad \sqrt{n}\varepsilon^{\ n\ \frac{1}{2}} \tag{54b}$$

The incorporation of the field intensity on Re and Nu numbers is through the Richardson-Zaki exponent $n = n_0 - p(H/Ms)$. Applying the same procedure to the results

obtained in subsection Case of independent coefficients of Darcy-Forchheimer equation, the heat transfer coefficient can be scaled as:

$$h_w \quad \frac{\varepsilon^{\frac{n}{4}}}{(1 \quad \varepsilon)^{\frac{n}{4}}} \tag{55}$$

Comments of the magnetic field effects on the Re and Nu numbers

The expressions (52) to (55) indicate that Re increases while Nu decreases as the bed voidage is increased at fixed field intensity. The latter could seem strange, but the last results of eqs. (52b) and (55) explain that there is an augmentation of the heat transfer coefficient with the porosity increase since the exponents $n - 1/2$ and $n/4$ are always positive with a range of moderate field intensities. The porosity increase leads to increased gas convection, larger voids and as a result increased heat transfer coefficients. The field intensity increase leads to reduced bed expansions, *i. e.* to hindered growth of porosity, which affects both Re and Nu numbers. In general, the magnetic field effect on h_w is due to the control of the bed length scale with respect to the internal gas flow. In other words, the field controls the expansion of the voids of the beds and consequently the gas convection within them.

These above comments explain the upward branch of the curve in the upper half of fig. 6. The descending branch corresponds to strong fields, *i. e.* to slow bed expansions; slow growth of cavities and consequent formations of channels with preferably gas bypass.

Brief conclusions

The problem with the friction factor of magnetically stabilized beds is relevant to a more general problem of fluid-driven deformation of saturated porous media. The problem has been investigated with foams and fibrous beds [14, 17], but under compression due to the flowing fluid. The problem discussed here is just the opposite – *a bed expanding due to the fluid drag*. This allows to formulate a special problem:

Fluid flow though a deformable porous media (fluid drag driven deformation under a constant pressure drop. Really, this is a special case since any field orientations different from axial one do not allow this special condition to be created.

The main result of the present study is the fact that the length scales of the flow are proportional to the bed porosity. The particular value of the scaling exponent depends on the type of the model employed to describe the pressure drop across the bed. These models are macroscopic and do not consider the rheology of the granular medium. Actu-

ally, this requires a more deep analysis, which cannot be performed with the models discussed here.

The term porosity was used here under a *very strong simplification* of the physical situation that *presupposes a homogeneous bed expansion*. At a micro scale, where the fluid drag takes place, the bed consists of channels dividing deformable particle aggregates elongated along both the fluid flow and field lines. Obviously, this behaviour is a "self organization" of the porous medium in order to minimize the fluid drag exerted by the fluid.

The scaling estimated developed through experiments and models allow to develop basic relationships required for engineering design of MSB and to explain the existing data on bed-to-surface heat transfer.

Nomenclature

A_c – cross-sectional area of the bed, [m^2]
A_0 – coefficients in eq. (49), [–]
Ar – Archimedes number, [$d_p^3 \rho_g (\rho_p - \rho_g) g / \mu_g^2$], [–]
a – specific contact area of the packed bed, [m^2/m^3]
B – magnetic field induction, [T] (in fig. 7 the old dimension [gaus, Gs] is used as in the original source)
C_D – friction factor defined by eq. (3a), [–]
C_{ni} – diameter of the effective channel diameter in a deformed bed, [m]
C_{n0} – diameter of the effective channel diameter in the initial bed, [m]
C_{Di} – friction factor of a deformed bed in accordance with eq. (13a)
C_{D0} – friction factor of the initial bed at $U = U_{e1}$, in accordance with eq. (13a)
D – tube (pipe or column) diameter – see the context, [m]
D_{Hi} – hydraulic diameter of the deformed bed, [m]
D_{H0} – hydraulic diameter of the initial bed, [m]
d_{ci} – length scale of the deformed bed inaccordance with eq. (13a)
d_{c0} – length scale of the initial bed at $U = U_{e1}$ in accordance with eq. (13a)
d_p – particle diameter, [m]
F – inertia factor of Forchheimer's equation, [–]
f – friction factor, [–]
f_i – friction factor of deformed bed (at a given fluid velocity $U > U_{mf0}$, or more precisely $U > U_{e1}$), [–]
f' – friction factor defined by eq. (29b) (through the coefficients of the Forchheimer equation), [–]
f_0 – friction factor defined by eq. (2c), [–]
H – magnetic field intensity, [A/m]
h_{b0} – initial bed height, [m]
h_w – wall-to-bed heat transfer coefficients, [W/m^{2}K]
K – porous bed permeability, [m^2]
K_L, K_{L0} – factors defined by eq. (9), [–]
K_E, K_{E0} – factors defined by eq. (10), [–]
k – thermal conductivity, [W/mK]
L – length, [m]

L_i – current (deformed), bed length, [m]
L_0 – initial bed length, [m]
M – exponent in eq. (9), [–]
M_E – pre-factor in eq. (10), [–]
Ms – magnetization at saturation, [A/m]
N_i – numbers of channels with a diameter C_{ni} (deformed bed), [–]
N_0 – numbers of channels with a diameter C_{n0} (non-deformed bed), [–]
Nu – Nuselt number (see the context for the specifically defined length scale l_0 and conductivity k), ($h_w l_0 / k$)
n – Richardson-Zaki exponent of a magnetizable bed, [–]
n_0 – Richardson-Zaki exponent of a non-magnetic bed, [–]
Pr – Prandtl number, (= $\mu c_p/k$), [–]
ΔP – pressure drop across the bed, [Pa]
p – pre-factor in eq. (17), [–]
R_c – ratio defined by eq. (7a), [–]
R_d – length scale ratio defined by eq. (13b), [–]
R_ξ – ratio defined by eq. (7b), [–]
Re – Reynolds number (see the context for the specifically defined length l_0 and velocity U_0 scales), (= $U_0 l_0/\nu$), [–]
Re_p – particle Reynolds number, eq. (5a), ($\rho_p U d_p / \mu_g$), [–]
S – fluid-particle contact area or wetted surface (see the context), [m^2]
U – superficial fluid velocity, [m/s]
U_{e1} – velocity at the onset of the stabilized bed, [m/s]
U_{e2} – velocity at the break-down of the stabilized bed, [m/s]
U_{mf} – minimum fluidization velocity, [–]
U_{mf0} – minimum fluidization velocity in absence of magnetic field, [m/s]
U_c – characteristic velocity, [= $-(dP/dx)K/\mu_f$], [m/s]
U_t – particle terminal velocity, [m/s]
V_0 – wetted volume of the initial bed, [m^3]
V_i – wetted volume of the deformed bed, [m^3]
x – axial co-ordinate (parallel to fluid flow and field lines, [m]

Greek letters

α_{eff} – effective thermal diffusivity, [m^2/s]
ε – porosity, [–]
ε_0 – porosity of the initial (non-deformed) bed, [–]
ε_i – porosity of the deformed bed, [–]
$\Delta\varepsilon_i$ – porosity increment due to the bed deformation, [–]
ξ – friction factor defined by eq. (3b), [–]
ξ_i – friction factor of a deformed bed according to eq. (3b), [–]
ξ_0 – friction factor of the initial bed at $U = U_{e1}$, in accordance with eq. (3b), [–]
μ – fluid dynamic viscosity, [Pa·s]
ν – fluid kinematic viscosity, [m^2/s]
Π_0 – wetted perimeter (of the cross-sectional area) of the initial bed, [m]
Π_i – wetted perimeter (of the cross-sectional area) of the deformed bed, [m]
ρ – density, [kg/m^3]
Φ – porosity function defined by eq. (6)
Ψ – undefined function, eq. (8), [–]

Subscripts

eff – effective
f – fluid
g – gas
p – particle
s – solid phase

Abbreviations

ID – Internal diameter
MFAF – Magnetic field assisted fluidization
MSB – Magnetically stabilized bed

References

[1] Hristov, J. Magnetic Field Assisted Fluidization – A Unified Approach, Part 1, Fundamentals and Relevant Hydrodynamic of Gas-Fluidized Beds, *Reviews in Chemical Engineering, 18* (2002), 4-5, pp. 295-509

[2] Hristov, J. Y., Expansion Scaling and Elastic Moduli of Gas-Fluidized Magnetizable Beds, in: Current Issues on Heat and Mass Transfer in Porous Media, NATO ASI "Emerging Technologies and Techniques in Porous Media " (Eds. D. Ingham, A. Bejan, E. Mamut, I. Pop), Kluwer, Dordrecht, UK, 2004, pp. 477-489

[3] Wentz, C. A., Thodos, G., Pressure Drop in the Flow of Gases through Packed and Distended Beds of Spherical Particles, *AIChE J.*, *9* (1963), 3, pp. 81-84

[4] Wentz, C. A., Thodos, G., Total and Form Drag Friction Factors for the Turbulent Flow of Air through Packed and Distended Beds of Spherical Particles, *AIChE J.*, *9* (1963), 3, pp. 358-361

[5] van der Merwe, D. F., Gauvin, W. H., Pressure Drag Measurements for Turbulent Air Flow through a Packed Bed , *AIChE J.*, *17* (1971), 2, pp. 402-407

[6] Hristov, J., Magnetic Field Assisted Fluidization – A Unified Approach. Part 2. Solids Batch Gas-Fluidized Beds: Versions and Rheology*, Reviews in Chemical Engineering, 19* (2003), 1, pp.1-132

[7] Penchev, I., Hristov, J., Behaviour of Fluidized Beds of Ferromagnetic Particles in an Axial Magnetic Field, *Powder Technology*, *61* (1990), 3, pp. 103-118

[8] Richardson, J. F., Zaki, W. N., Sedimentation and Fluidization, Part I, *Trans. I Chem. Eng.*, *32* (1954), 1, pp 35-50; see also *Trans. I Chem. Eng.*, *75* (1997), S82

[9] Rosensweig, R. E., Fluidization: Hydrodynamics Stabilization with a Magnetic Field, *Science, 204* (1979), 6, pp. 57- 60

[10] Foscolo, P. U., Gibilaro, L. G., Di Felice, R., Waldram, S. P.,The Effect of the Interparticle Forces on the Stability of Fluidized Beds, *Chem. Eng. Sci. 40* (1985), 12, pp.2379-2381

[11] Beek, W. J., Mutzall, K. M. K., Transport Phenomena, John Wiley and Sons, Bristol, 1975

[12] Denn, M. M., Process Fluid Mechanics, 1st ed., Prentice-Hall, Englewood Cliffs, NJ., USA, 1980

[13] Beavers, G. S., Sparrow, E. M., Rodenz, D. E., Influence of Bed Size on the Flow Characteristics and Porosity of Randomly Packed Beds of Spheres, *J. Appl. Mech*, *40* (1973), 9, pp. 655-660

[14] Beavers, G. S., Wilson, T. A., Masha, B. A., Flow Through a Deformable Porous Material, *J. Appl. Mech*, *42* (1975), 9, pp. 598-602

[15] Ward, J. C., Turbulent Flow in Porous Media, *J. Hidraul. Div.A. Soc.Civ.Eng.*, *90* (1964), HY5, pp. 1-12

[16] Joseph, D. D., Nield, D. A., Papanicolaou, Non-Linear Equation Governing Flow in a Saturated Porous Medium, *Water Res. Research*, *18* (1982), 4, pp. 1049-1052
[17] Beavers, G. S., Sparrow, E. M., Compressible Gas Flow through a Porous Material, *Int. J. Heat Mass Transfer, 14* (1971), 11, pp. 1855-1899
[18] Geldart, D., Types of Gas Fluidization, *Powder Technology, 7* (1973), 2, pp. 285-292
[20] Philippow, E., Nonlinear Electrotechnic (in German), Leipzig, German DR, 1971 (there is a Russian translation by Energia publishing, Moscow, 1976)
[21] Hristov, J. Y., Comments on Gas-Fluidized Magnetizable Beds in a Magnetic Field, Part 3: Heat transfer, *Thermal Science, 4* (2000), 1-2, pp. 3-48
[22] Hristov, J. Y., Magnetic Field Assisted Fluidization – A Unified Approach, Part 3, Heat Transfer – A Critical Re-Evaluation of the Results, *Reviews in Chemical Engineering, 19* (2003), 3, pp. 229-355
[23] Hristov, J. Y., Fluidization of Ferromagnetic Particles in a Magnetic Field, Part 1: The Effect of the Field Lines Orientation on Bed Stability, *Powder Technology*, *87* (1996), pp. 59-66
[24] Beckerman, C., Viskanta, R., Forced Convection Boundary Layer Flow and Heat Transfer along a Plate Embedded in a Porous Medium, *Int. J. Heat Mass Transfe, 30* (1987), 7, pp. 1547-1551
[25] Kaviany, M., Mittal, M., Natural Convection Heat Transfer from a Vertical Plate to High Permeability Porous Media: an Experiment and Approximate Solution, *Int. J. Heat Mass Transfer, 30* (1987), 5, pp. 967-977
[26] Arnaldos, J., A Study on Stabilization of Gas-Fluidized Beds Subjected to the Action of a Magnetic Field (in Spanish), Ph. D. thesis, Univ. Politechnica de Catalunya, Barcelona, Spain, 1986
[27] Neff, J., Rubinsky, B., The Effect of a Magnetic Field on the Heat Transfer Characteristics of an Air Fluidized Bed of Ferromagnetic Particles, *Int. J. Heat Mass Transfer, 16* (1983),12, pp. 1885-1889
[28] Hristov, J. Y., Heat Transfer between Deformable Magnetic Beds and Immersed Surfaces: Cases of Gas-Fluidized Beds, *Proceedings*, Thermal Sciences 2004 (Eds. A. Bergles, I. Golobic, Cr. Amon, A. Bejan), ASME-ZSIS International Thermal Science Seminar ITSS II, Bled Bled, Slovenia, June 13-16, 2004, pp. 267-274

Author's address:

J. Y. Hristov
Department of Chemical Engineering
University of Chemical Technology and Metallurgy
1756 Sofia, 8 Kl. Ohridsky Blvd., Bulgaria,

e-mail: jyh@uctm.edu; jordan.hristov@mail.bg
Website: http://hristov.com/jordan

Paper submitted: March 29, 2004
Paper revised: January 11, 2005
Paper accepted: February 15, 2005